Diffusing-wave-spectroscopy investigation of latex particle motion in polymer gels

G. Nisato,* P. Hébraud, J.-P. Munch, and S. J. Candau
Laboratoire de Dynamique de Fluides Complexes, 3 rue de l'Université, 67084 Strasbourg, France
(Received 1 February 1999; revised manuscript received 5 November 1999)

Dynamic light scattering studies of particle motion in cross-linked chemical gels are limited by the fact that when the cross-linking ratio is increased, the scattered intensity becomes quenched, and time-dependent concentration fluctuations contribute less and less to the overall scattering signal. The concentration fluctuations then occur at very small length scales, which can become inaccessible to classical dynamic light scattering techniques. Diffusing wave spectroscopy can help overcome these experimental difficulties. We extend this technique to the case of nonergodic systems, and apply it to the detection of the motion of probe particles trapped inside chemically cross-linked gels. We measure the mean square displacement of the nanometric probes, leading to the measurement of local mechanical properties of the gel matrix.

PACS number(s): 83.85.Ei, 83.10.Dd, 82.70.Gg

I. INTRODUCTION

Microrheological techniques have been applied to the study of soft-matter systems since the late 1920s, and have recently received an increasing amount of interest, both from experimental and theoretical points of view [1–6]. The main advantage of these techniques resides in the fact that they allow an *in situ* determination of the rheological properties of a wide range of materials extending the dynamic range of classical rheometers as well as the type of systems, synthetic or biological, that can be studied. Recently, several works focused on ''passive'' microrheological techniques [4,5,7]. In this kind of approach, thermal fluctuations drive the motion of probe particles embedded in the medium being studied. By measuring either the mean square displacement or the power spectrum of the position fluctuations of the probe particles, it is possible to calculate the mechanical response of the medium. A classic example is given by the Brownian motion of latex spheres suspended in a Newtonian fluid: the Stokes-Einstein relationship relates the mean square displacement of the particles to the viscosity of the medium, which can be thus measured once the particle size is known.

When the medium surrounding the probe particles is elastic (i.e., has a nonzero storage modulus at zero frequency), the elementary theory of elasticity states that the particles are geometrically confined. The inherent nonergodicity of these systems has to be addressed when light scattering techniques are used to measure the motion of probe particles. In this paper we address this point by extending the formalism that was developed for interpreting dynamic light scattering in nonergodic media to the case of diffusing wave spectroscopy, and we also report the results of a study on a model nonergodic system.

The study of the dynamics of nonergodic systems is made difficult by the fact that they explore only a fraction of all their possible configurations. More specifically, the experimentalist who wants to investigate the domain of the phase space that is actually explored by the system and its associated dynamics encounters two main difficulties. First of all, ensemble averages over all the configurations have to be performed explicitly by the observer. Second, the length scales freely explored by the system are limited, and therefore it is necessary to perform observations at short time and length scales.

Polymer gels are a very good example of nonergodic systems. In these materials, the concentration fluctuations are geometrically and topologically constrained by the presence of cross-links that act as a quenched disorder. The dynamic properties of polymeric gels have been investigated using dynamic light scattering (DLS), which probes the time-dependent density fluctuations occurring in the scattering volume under observation [8–10]. The scattered intensity is found to be the sum of a random thermal component and a quenched term that depends on the location of the scattering volume inside the gel [11]. The intensity associated with the frozen-in component depends in a complex manner on the conditions of preparation of the gel. More specifically, it is related to the polymer concentration and to the cross-linking ratio, defined as the molar ratio of cross-linking units to the total number of monomers.

Upon increasing the cross-linking density, the thermal motion of the scatterers becomes more and more hindered, and one needs to probe the system at smaller and smaller length scales to detect any motion or relaxation phenomena. Eventually, the scale of observation is no longer accessible to DLS, and one must turn to other techniques of investigation. Diffusing wave spectroscopy (DWS), an extension of the light scattering technique suited for the study of highly scattering systems, allows one to probe displacements of the scatterers of the order of a few angstroms. This is due to the fact that the phase shift between an entering and an exiting photon results from a large number N of scattering events. The motion of each of the scatterers over a distance of the order of λ/N is enough to completely decorrelate the scattered signal [12]. The motion of latex spheres suspended in water and polymer solutions at length scales as small as few angstroms has been investigated using this technique [13].

In the present study we consider covalently cross-linked gels containing nanometric polystyrene spheres with diameter much larger than the mesh size ξ ($\sim$ 5 nm) of the poly-

*Present address: Philips Research, Prof. Holstlaan 4 (WB72), NL-5656 AA Eindhoven, The Netherlands.

mer network. The distance over which the particles can move in a polymer matrix is controlled by the competition between the thermal energy and the elasticity of the matrix. As the cross-link density is increased, the elasticity of the polymer network increases, leading to increasingly smaller spatial excursions of the particles, that eventually cannot be detected by DLS. The amplitude of the mean square displacement of each bead is limited and reaches a finite value, $\Delta r^2(\infty)=6\delta^2$, at long times. Thus, when probing the motion of the beads at length scales larger than δ, one can observe the effect of nonergodicity of the system: the result of a given light scattering experiment depends on the particular scattering volume observed or, equivalently, on the particular point of the speckle pattern being observed. One therefore needs to perform an ensemble average in order to obtain thermodynamically relevant quantities. The simplest and most efficient, but also must tedious method, consists of performing the ensemble average ''manually,'' by measuring the desired quantities for a great number of different configurations and then properly averaging them. However, it is possible to find relationships between measured time averaged and ensemble averages of interest. Pusey and Van Megen derived such relationships in the case of DLS [14]. In the first part of this paper we show that the same approach can be extended to DWS. We then experimentally investigate the dynamics of latex beads embedded in chemically cross-linked polyacrylic acid gels. By varying the cross-link density, one can tune the elastic modulus G in a rather large range ($\sim 10\,\mathrm{Pa}<G\leqslant 10^3\,\mathrm{Pa}$). We took advantage of this possibility to determine the ranges of G for which either DLS or DWS can be used, thus showing the complementary character of these two techniques to probe the motion of the particles trapped in polymer gels over a large gamut of length scales.

II. DWS IN NONERGODIC SYSTEMS

The following presentation requires a certain familiarity with the DWS formalism presented by Weitz and Pine in Ref. [12] as well as the work of Pusey and Van Megen [14]. We took advantage of the following analogies: one optical path in DWS plays the role of a single scatterer in DLS, and one distribution of paths in DWS plays the role of one scattering volume in DLS.

Let us consider a plane wave traveling through a medium turbid enough for the phase of an entering photon to be randomized when it leaves the sample. In other words, we state that each photon follows a random walk inside the medium [15]. The electric field $\mathbf{E}(\mathbf{r}_0,t)$ at the output of the sample can be written

$$\mathbf{E}(\mathbf{r}_0,t)=\sum_{p\in P}\mathbf{E}_0 e^{i\Phi^p(t)}=\sum_{p\in P}\mathbf{E}^p, \tag{1}$$

where P is the ensemble of optical paths that begin at the entering surface of the sample and ends at a point $\mathbf{r}_0$ on the detector, $\mathbf{E}_0$ is the incident electric field, $\Phi^p(t)$ is the phase difference due to diffusion along path p inside the sample, and $\mathbf{E}^p$ is the electric field associated with path p. The expression of the electric field is similar to the one encountered in DLS,

$$\mathbf{E}(\mathbf{q},t)=\sum_{r_j\in V_{\mathrm{diff}}}\mathbf{E}_0 e^{i\mathbf{q}\mathbf{r}_j(t)}, \tag{2}$$

where $\mathbf{r}_j$ are the positions of the scatterers belonging to the observed diffusing volume V_{diff}, and $\mathbf{q}$ is the transfer vector. However, Eqs. (1) and (2) differ in two aspects. In DWS, the expression of the phase difference is a sum over a large number of scattering events, whereas only one scattering event occurs in DLS. Also, in DLS one does not have any *a priori* information about the spatial correlation of the individual scatterers ($\mathbf{r}_j$), whereas in DWS one may assume that two optical paths are not correlated [12]. As we will see further, the last property simplifies the expression of the dynamic structure factors. It also leads to a linear relationship between the correlation function of the electric field associated with path p and the correlation function of the total electric field, which simplifies the computation of the latter [12].

We now focus our attention on the expression of the intensity scattered at one point $\mathbf{r}_0$ of the output. As all the paths are independent we have

$$I(t)=\sum_{p\in P'}\mathbf{E}^p(t)\cdot\mathbf{E}^{p*}(t). \tag{3}$$

If the system is ergodic, then $\Phi^p(t)$ is a random variable as well as $\mathbf{E}^p(t)$. The total electric field $\mathbf{E}(t)$ is then a Gaussian variable, according to the central limit theorem. Therefore the ensemble-averaged correlation function of the intensity may be factorized according to [16]:

$$\langle\langle I(t)I(t+\tau)\rangle_t\rangle_\varepsilon=\langle I(t)\rangle_\varepsilon+[F(t)]^2, \tag{4}$$

where

$$F(\tau)=\sum_p\sum_{p'}E_0^2\langle\langle\exp[i\Phi^p(t)-i\Phi^{p'}(t+\tau)]\rangle_t\rangle_\varepsilon. \tag{5}$$

Since no correlation exists between any two given paths, the ensemble average in Eq. (5) is redundant, as it is performed by the summation over the paths; hence

$$F(\tau)=\sum_p E_0^2\langle\exp[i\Phi^p(t)-i\Phi^p(t+\tau)]\rangle_t=\langle I\rangle_\varepsilon f(\tau). \tag{6}$$

By definition [14], $f(\tau)$ is the normalized dynamic structure factor function. This relationship is of crucial importance as it links an ensemble-averaged function to a time-averaged observation at one given point, which is position dependent. It lies in the fact that all the optical paths have been assumed to be noncorrelated.

Let us now consider a nonergodic medium. We assume that each particle can move around a fixed position $\mathbf{R}_j$, so that its position may be written

$$\mathbf{r}_j(t)=\mathbf{R}_j+\boldsymbol{\delta}_j(t) \tag{7}$$

where $\langle\boldsymbol{\delta}_j(t)\rangle_t=0$, so that the phase difference $\Phi^p(t)$ along path p may be decomposed in the same way:

$$\Phi^p(t)=\Psi_c^p+\Phi_f^p(t). \tag{8}$$

The first term in Eq. (8) is time independent, and the mean value of the second one is zero. We are thus allowed to write

$$\mathbf{E}^p(t)=\mathbf{E}_c^P+\mathbf{E}_f^p(t) \tag{9}$$

where, if we put $w^p=\langle\exp[i\Phi_f^p(t)]\rangle_t$, the fixed and the fluctuating components of the electric field are

$$\mathbf{E}_c^P=\mathbf{E}_0\exp(i\Psi_c^p), \tag{10}$$

$$\mathbf{E}_f^P(t)=\mathbf{E}_0\exp(i\Psi_c^p)[\exp(i\phi_f^p)-w^p]. \tag{11}$$

The total electric field is the sum of a constant field and a Gaussian field:

$$\mathbf{E}(t)=\sum_{p\in P}\mathbf{E}^p(t)=\sum_{p\in P}\mathbf{E}_c^P(t)+\sum_{p\in P}\mathbf{E}_f^P(t). \tag{12}$$

Equation (12) describes a heterodyne DLS experiment, in which a reference field is superimposed to the field of scattered radiation [17]. In our case, the ''reference'' and the oscillating sources are a consequence of the nonergodicity of the physical system, leading to a self-heterodyne situation [8].

The experimentally accessible quantity is the time-averaged autocorrelation function of the scattered intensity, which can be expressed as [17]

$$\langle I(t)I(t+\tau)\rangle_t=\langle I_f(t)I_f(t+\tau)\rangle_t+2I_c\langle\mathbf{E}_f(t)\cdot\mathbf{E}_f^*(t+\tau)\rangle_t+2I_c\langle I_f(t)\rangle_t+I_c^2, \tag{13}$$

where I_f and I_c are the fluctuating (time-dependent) and the frozen-in components of the scattered intensity, respectively. The first two terms of Eq. (13) may be evaluated using the Gaussian character of $\mathbf{E}_f(t)$, leading to:

$$\langle\mathbf{E}_f(t)\cdot\mathbf{E}_f^*(t+\tau)\rangle_t=\langle I\rangle_\varepsilon[f(\tau)-f(\infty)], \tag{14}$$

$$\langle I_f(t)I_f(t+\tau)\rangle_t=\langle I\rangle_\varepsilon^2[I-f(\infty)]^2+[f(\tau)-f(\infty)]^2. \tag{15}$$

Most commercially available autocorrelators measure the normalized time-averaged autocorrelation function of the scattered intensity: $g_t^2(\tau)=\langle I(t)I(t+\tau)\rangle_t/\langle I(t)\rangle_t^2$, which is linked to the structure factor $F(\tau)$ through

$$g_t^2(\tau)=1+Y^2[f(\tau)^2-f(\infty)^2]+2Y(1-Y)[f(\tau)-f(\infty)], \tag{16}$$

where $Y=\langle I\rangle_\varepsilon/\langle I\rangle_t$. We remind the reader that $\langle I\rangle_t$ depends on the on the spot of the speckle pattern being observed. This relationship between time-averaged autocorrelation function and dynamic structure factor expressed in Eq. (16) was established by Pusey and Van Megen in the case of DLS, and discussed in detail in Ref. [14].

If we assume now that the mean temporal value of the intensity does not depend on the observation point, we obtain

$$(g_t^2(0)-1)\langle I(t)\rangle_t^2=-I_f^2+2\langle I(t)\rangle_t I_f. \tag{17}$$

TABLE I. Fitting parameters and estimated local rheological quantities [see Eqs. (23) and (24)] corresponding to different crosslinking ratios R_c. DLS and DWS data were obtained with particles having diameters of 85 and 107 nm, respectively.

	R_c	δ^2 (nm^2)	$\langle\tau_c\rangle$ (ms)	γ	v (Pa s)	μ (Pa)
DLS	1.6×10^{-3}	390	144	0.52	1.9	10
	2×10^{-3}	250	89.2	0.47	1.8	16
	5×10^{-3}	26	14.4	0.31	2.9	150
DWS transmission	5×10^{-3}	16	8.89	$\leqslant$0.3	2.3	250
DWS backscattering	1×10^{-2}	2.6	0.79	$\leqslant$0.3	1.2	1500

The left-hand side is thus a linear function of $\langle I(t)\rangle_t$, and its slope is $2I_f$. This equation allows a direct way to check experimentally the ''self-heterodyning'' of the scattering. It also provides an accurate method to measure I_f and to show it is not dependent on the sample position.

III. RESULTS AND DISCUSSION

A. Sample preparation

We studied the motion of latex particles embedded in gel matrices chemically cross-linked to different degrees. The probe particles were latex particles (Poly Science nanospheres), their diameters were measured by DLS in water suspensions at a volume fraction $\phi=2.5\times10^{-2}$. We used 85-nm particles for the samples studied by DLS, and 107-nm particles for the samples studied by DWS. The spheres occupied volume fractions $\phi=10^{-4}$ and $\phi=2.5\times10^{-2}$ in the samples studied by DLS and DWS, respectively. The gel matrices were polyacrylic acid (PAA) gels. The total polymer concentration $C_p=0.05$ g/cm^3 was kept constant in all the samples. The cross-linking ratio R_c, defined as the molar ratio of cross-linking molecules to the total molar monomer concentration, varied from 1.6×10^{-3} to 1×10^{-2} (see Table I). The samples were prepared by radical copolymerization of acrylic acid and methylene bis-acrylamide monomers in aqueous solutions containing the appropriate volume fraction of polystyrene nanospheres. The radical polymerization reaction, performed at 70 °C, was initiated by the addition of addition of ammonium persulfate immediately after the solutions were degassed. The samples were prepared directly in the light scattering cells. The sample preparation was performed along the lines of the experimental protocol detailed in previous publications, where further details can be found [18].

The polymer network thus formed is weakly anionic, reducing the risk of physisorption on the surface of the latex particles, since the latter are lightly sulfonated. For the polymer concentrations under consideration, it is possible to estimate an average ''mesh size'' ξ of the polymer network of the order of 5 nm, much smaller than the diameter of the probe particles [19]. The polymer matrix can therefore, in a first approximation, be considered as a continuous medium at the length scale of the nanospheres.

B. Experimental setup

1. DLS

The coherent source was a Spectra Physics 2020 laser, operated at 0.4 W with $\lambda = 488$ nm. The correlation functions were calculated by an ALV 5000 logarithmic autocorrelator (in the ''Single'' mode). The coherence factor of the experimental setup was measured with a reference latex suspension and corresponded to $\beta = 0.97 \pm 0.02$. All the experiments were performed in a controlled environment at $22\,^{\circ}\mathrm{C} \pm 0.5$. The scattering cells were vertically translated with a PC-controlled step motor (Microcontrole), allowing reproducible positioning with a resolution of 1 μm. The total excursion was 7 mm. For each sample and scattering angle, we measured 1000 different autocorrelation functions of the scattered intensity (10-s acquisition time for each one of them) in order to calculate the ensemble-averaged dynamic structure factor [9,10,14,20].

2. DWS

The coherent source was a Spectra Physics 2020 laser, operated at $\lambda = 488$ nm. The laser beam was expanded to approximately 1 cm at the sample. The diffused light was collected by two monomode optic fibers (ALV) connected to ALV photon-counting devices. One of the fibers was placed in the axis of the beam (''transmitting'' geometry), and the second fiber was placed in the backscattering cone (''backscattering'' geometry).

The characteristic length scales probed by DWS in the ''backscattering'' and ''transmitted'' geometries are defined by $l_B^2 = [1/k_0^2(z_0/l^* + 2/3)^2]$ and $l_T^2 = (l^*/k_0 L)^2$, respectively, where $k_0^2 = 2\pi/\lambda$, $L = 0.5$ mm is the thickness of the sample, $l^* = 140$ μm is the scattering mean free path, and z_0 is the penetration depth [15]. The relationships above are obtained by expanding at long times the properly normalized expressions for the dynamic structure factors in DWS which can be found in Ref. [15]. The lengths l_B and l_T are the equivalent of the inverse scattering vector q in the DLS experiments, and one has $l_B \ll l_T$. Therefore, these two observation geometries allow us to probe relaxation phenomena occurring at two different length scales. From experiments performed on latex suspensions in water, we obtained $l_B = 2.3$ nm and $l_T = 16$ nm.

The sample was either translated by a PC-controlled step-motor analogous to the one employed in the DLS setup, or was displaced with an electroacoustic [21] device. In the second case the sample is translated at a frequencies between 60 and 100 Hz, the amplitude of the oscillatory motion being on the order of 1 mm.

We used two different types of correlators. For the determination of the dynamic structure factor, following the same protocol as in DWS we used the ALV 5000 correlator. For the correlation echo technique we used a BI 9000 correlator, which can be configured in such a way as to concentrate a great number of correlation channels around the delay times coinciding with the peak positions, thus allowing their measurement with a good precision [21].

C. Experimental results and discussion

Figure 1(a) shows the dynamic structure factor of a gel whose cross-linking ratio is 2×10^{-3}. This is a typical case

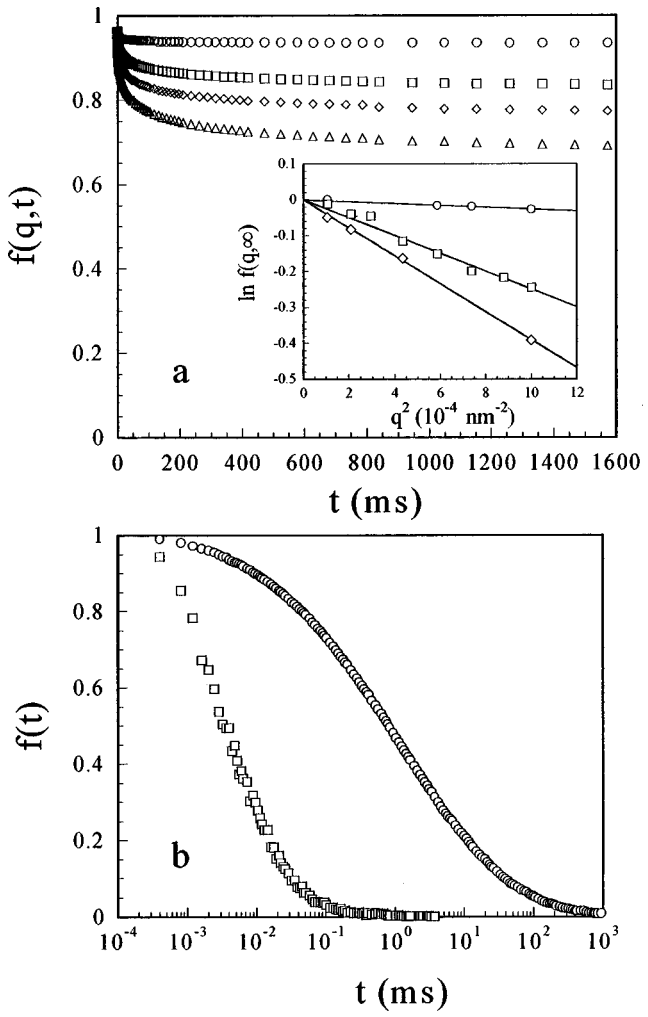

FIG. 1. (a) Dynamic structure factors for a gel ($R_c = 2 \times 10^{-3}$, $C_p = 0.05$ g/cm^3) containing polysterene nanospheres (85 nm) at a volume fraction $\phi = 10^{-4}$. The different curves correspond to scattering angles of 35° (open circles), 75° (open squares), 105° (open diamonds), and 135° (open triangles). The inset shows the q^2 dependence of the limiting value of the dynamic structure factor at long times, $f(q,\infty)$. Data sets correspond to gels having the same concentration and volume fraction of particles as above; cross-linking ratios are equal to 5×10^{-3} (circles), 2×10^{-3} (squares), and 1.6×10^{-3} (triangles). Note that the values of the y axis are logarithmic. Solid lines are linear least-squares fits to the data [cf. Eq. (18)]. (b) Dynamic structure factor of an equivalent sample ($R_c = 2 \times 10^{-3}$, and $C_p = 0.05$ g/cm^3 and 107-nm particles at $\phi = 2.5 \times 10^{-2}$) as measured by DWS in the transmitted (squares) and backscattering (circles) geometries.

for which DLS and DWS measurements are complementary. Figure 1(a) displays the q variation of the dynamic structure factor as measured by DLS. Whatever the magnitude of the wave vector transfer q, the structure factor does not go to zero when time goes to infinity but reaches a nonzero asymptotic value which depends on the value of q. Following Ref. [14], we took

$$\lim_{t \to \infty} f(q,t) = e^{-q^2 \Delta r^2(\infty)/6} = e^{-q^2 \delta^2}. \tag{18}$$

As illustrated in the inset of Fig. 1(a), where the data collected for cross-linking ratios $R_c = 1.6 \times 10^{-3}$ and $R_c = 5$

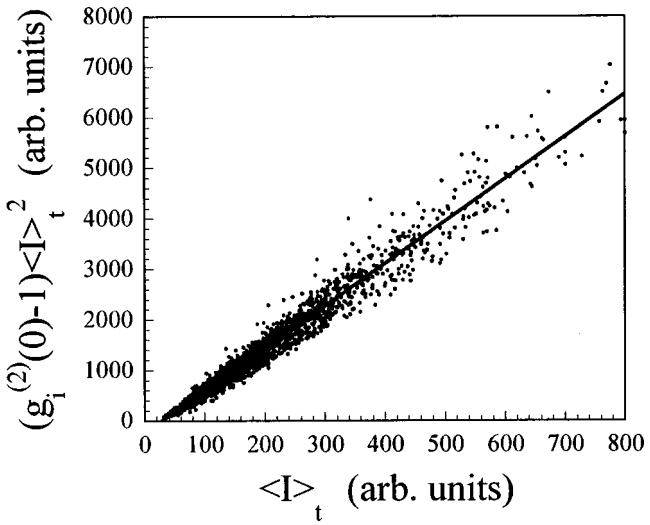

FIG. 2. Experimental verification of the ''self-heterodyne'' relationship [cf. Eq. (18)] in DWS (backscattering geometry). On the x axis are plotted the total scattering intensities (time-averaged) corresponding to a total of 2000 observation points, plotted on the graph. The sample is a gel with $R_c=1\times10^{-2}$, $C_p=0.05\ \mathrm{g/cm^3}$, and $\phi_o=2.5\times10^{-2}$. The solid line is a least-squares linear fit to the data; the slope is proportional to the fluctuating component of the scattered intensity [cf. Eq. (17)].

$\times10^{-4}$ are also presented, the experimental results can be fitted very satisfactorily with Eq. (17), leading to the determination of the characteristic spatial length explored by the particles, δ, as a function of the cross-linking ratio (cf. Table I). However, to better determine the dynamics of the bead inside this Brownian cage, one needs probe smaller length scales. Figure 1(b) represents the dynamic structure factors obtained from the DWS intensity correlation functions on sample similar to the one studied by DLS. We represented the measurements corresponding to the backscattering and transmission geometries. First of all, the measured structure factors go to zero at long times, both in the transmission and in the backscattering geometries, showing that the confinement of the particles cannot be seen at the scales probed by this technique. The dynamics of the particles at short length scales thus obtained shows a subdiffusive motion of the probes. In all the samples we studied, the motion of the particles was never purely diffusive, even at the shortest detection times.

We focus now on more strongly cross-linked systems, for which nonergodicity effects are apparent even in DWS. We performed series of autocorrelation experiments in which the sample was moved by steps of 200 μm, thus observing different points $\mathbf{r}_o$ of the speckle pattern. We first checked that general assumptions of our treatment were valid, by plotting $[g^2_{r_o}(0)-1]\langle I_{r_o}\rangle_t^2$ versus $\langle I\rangle_t^2$. Figure 2 shows the typical curve obtained by plotting 2000 data points, each one corresponding to a different position of the sample. The data are in very good agreement with the linear relationship [Eq. (17)]. This linear dependence was found in all the samples presenting a nonergodic behavior. Therefore, in this case the electric field of the scattered intensity can be decomposed into constant and Gaussian parts, and the time average of the fluctuating part of the intensity does not depend on the point of observation.

In spite of the fact that the latex particles embedded in the gels are strong light scatterers, in DLS experiments it is not possible to neglect the component of the intensity associated with the polymer concentration fluctuations of the bare gel, I_{PAA} [22].

The dynamic structure factors obtained by DLS were fitted with a nonlinear least-squares fitting procedure using the expression

$$f(q,t)=f(q,\infty)+A\exp(-t/\tau_{\mathrm{PAA}})+[(1-A-f(q,\infty)]\exp[-(t/\tau_c)^{\gamma}]. \quad (19)$$

This functional form was chosen primarily because it allows for quick, reproducible and satisfactory fits of the data, as illustrated by Fig. 3(a). The amplitude parameter A is the ratio between the scattering intensity associated with the concentration fluctuations of the gel and the fluctuating part of the scattering intensity associated with the motion of the probe particles I_F, i.e., $A=I_{\mathrm{PAA}}/I_F$; τ_c and τ_{PAA} are the correlation times associated with the particle motions and the polymer concentration fluctuations of the gel, respectively. As illustrated in Fig. 3(b), the values of τ_{PAA} measured in the different gels are in good agreement with those measured in an equivalent solution at the same concentration of the gel (crosses), showing the usual q^{-2} dependence [9,23–25].

The values of the exponent of the stretched exponential, γ, reported in Table I, are essentially independent on the scattering vector for a given system, but depend systematically on the cross-linking ratio. The evolution of γ with cross-linking ratio could bear relevance to theoretical work on relaxation phenomena in disordered media. The evolution of the exponent could be related to the increasing amount of frozen-in disorder in the gel matrix surrounding the probe particles [26]. This ''disorder'' ought to be an increasing function of the cross-liking ratio, as the degrees of freedom of the polymer concentration fluctuations are increasingly hindered by the presence of physical links between neighboring chains. In order to compare the characteristic times τ_c corresponding to different values of γ, we followed Delsanti and Munch in Ref. [27] and calculated the averaged time: $\langle\tau_c\rangle=\Gamma(\gamma)\tau_c/\gamma$, where Γ is the Eulerian gamma function.

The correlation time τ_c can be viewed as the characteristic exploration time of the Brownian cage, i.e., the time each particle will require to explore a significant portion of its allowed positions. This correlation time ought to be independent on the *observation* scale q^{-1}. Figure 3(b) clearly illustrates this point for our experimental systems. The values of δ^2 and $\langle\tau_c\rangle$ as obtained from the above analysis are reported in Table I.

As the cross-linking ratio increases, the average mean square displacement decreases and eventually can no longer be detected reliably using DLS. The main motivation for using DWS is then to expand the range of detection to smaller displacements.

In Fig. 4 we show the dynamic structure factors obtained in the backscattering and transmission geometries, for cross-linking ratios of 5×10^{-3} [Fig. 4(a)] and 10^{-2} [Fig. 4(b)]. We now see that the structure factor reaches a nonzero value at long times, from which we can deduce the maximum mean square displacement of the particles, according to

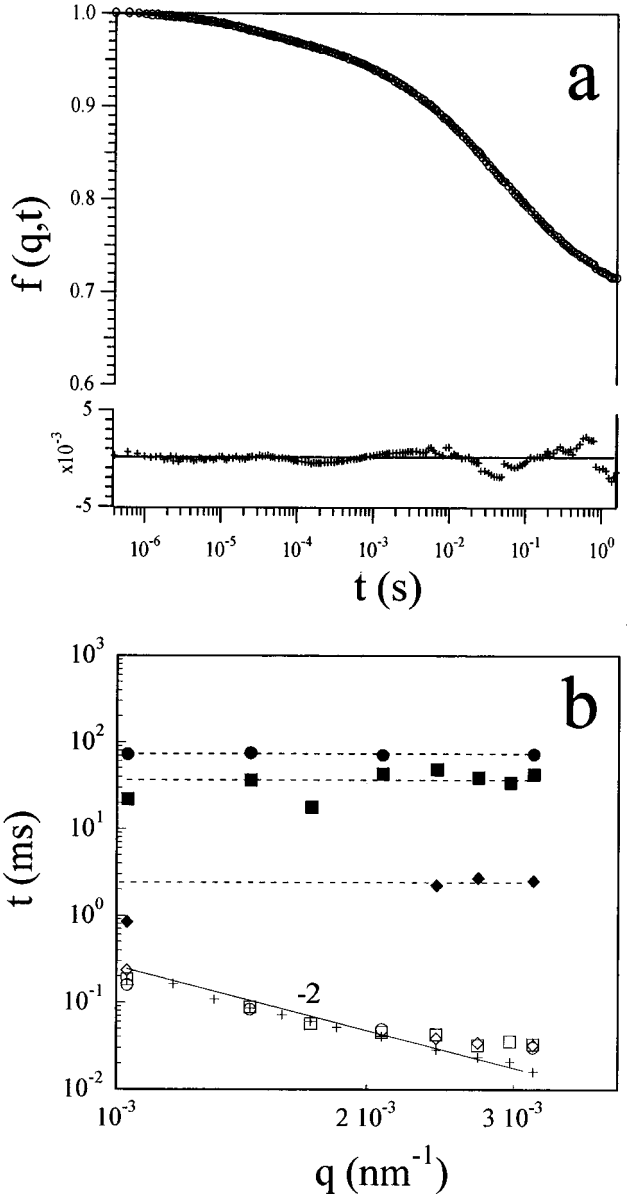

FIG. 3. (a) Example of DLS dynamic structure factor [$R_c=2.2\times10^{-3}$, $C_p=0.05$ g/cm^3, and $\phi_.=1\times10^{-4}$ (85-nm latex spheres), and the scattering angle is 90°]. The decay function is bimodal. The solid line is a least-squares nonlinear fit to the data using Eq. (19). The residual plot of the fit is shown on the bottom of the figure. Note that the maximum deviation is less than 3%. (b) Variation of the characteristic decay times associated with the ''cage'' dynamics, τ_c, and with the polymer concentration fluctuations of the gel, τ_p, as a function of the magnitude of the scattering vector q. Filled symbols correspond to the τ_c of gels with $C_p=0.05$ g/cm^3 at $\phi=10^{-4}$ (85-nm polystyrene nanospheres); cross-linking ratios are 5×10^{-3} (diamonds), 2×10^{-3} (squares), and 1.6×10^{-3} (circles). Open symbols show the evolution of τ_p for the corresponding gels. For comparison, the decay time measured on a PAA solution at the same concentration prepared in the same conditions (crosses) is also shown.

$$\text{backscattering} \quad \lim_{t\to\infty} f_B(t)=e^{-\delta^2/6l_B^2}, \tag{20}$$

$$\text{transmission} \quad \lim_{t\to\infty} f_T(t)=e^{-\sqrt{\delta^2/6l_T^2}}. \tag{21}$$

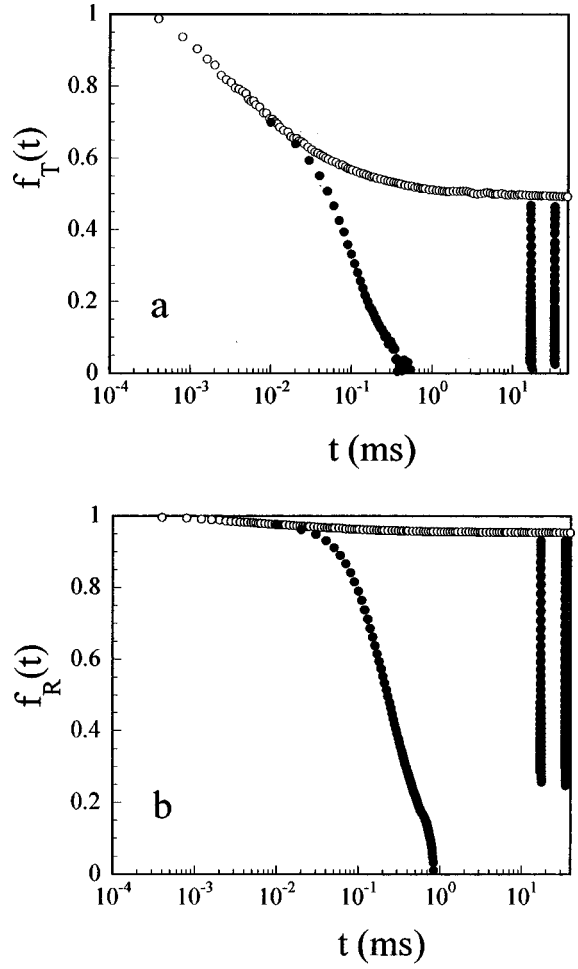

FIG. 4. (a) Dynamic structure factor of a gel measured by DWS in the transmitted geometry (open circles). Sample characteristics: $R_c=1\times10^{-2}$, $C_p=0.05$ g/cm^3, and $\phi_.=2.5\times10^{-2}$. Filled circles show the result of a correlation-echo experiment performed on the same sample. (b) DWS dynamic structure factors (open circles) and correlation echo (filled circles) for the same sample as in Fig. 3(a), but now in the backscattering geometry.

The values of δ^2 obtained by using the above expressions are reported in the table. In both cases, δ^2 would have been too small to be measured reliably using DLS.

Let us remark that this way of performing explicitly the ensemble averages is time consuming, and that at least one key quantity, namely the plateau value of the mean square displacement, can be obtained more readily by computing the intensity correlation function while the sample is in oscillatory motion. During one period, the light from a large number of different points of the speckle is collected, and the ensemble average over all these points is performed in real time. The shape of the correlation function reflects both the macroscopic motion of the sample and the dynamics of the beads themselves inside the gel. The filled circles in Figs. 4(a) and 4(b) show the results obtained in these experiments. One sees a first decrease due to the collective motion of the sample imposed by the translation, then a series of echoes, centered around the period of excitation (two echoes in the presented experiment), as the sample comes back periodically to the position it occupied one period before. Due to their random motion inside the gel matrix, the scatterers do

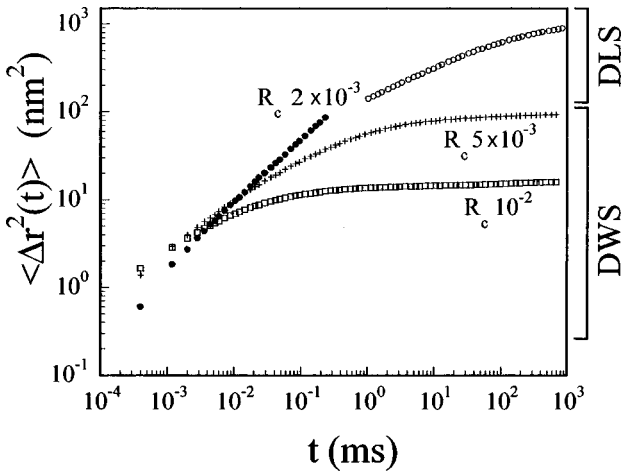

FIG. 5. Mean square displacement as a function of time for probe particles embedded in different gels matrices with $C_p = 0.05\ \mathrm{g/cm^3}$ and $\phi_o = 2.5\times10^{-2}$; the cross-linking ratios of the different samples are $R_c = 2\times10^{-3}$ (open and filled circles), $R_c = 5\times10^{-3}$ (plus signs) and $R_c = 1\times10^{-2}$ (squares). The spatial ranges accessible to DWS (backscattering) and DLS are shown on the right hand side. Open circles correspond to DLS measurements.

not come back exactly to their previous positions, and the height of the correlation echo is thus smaller than 1. In fact, we recover the value of the ensemble average structure factor at discrete times corresponding to integer multiples of the oscillatory frequency. Thus we are able to measure the maximum mean square displacement, provided that the period of the imposed translation is larger than the correlation time of the structure factor due to the motion of the beads around their average position.

Let us come back to the full structure factor. General DWS theory allows us to express it as a function of the ensemble averaged mean square displacement $\langle \Delta r^2(t) \rangle$ [12], from which we deduce, by a point to point numerical inversion of the formulas, the ensemble-averaged mean square displacement of the probe particles. The results are given in Fig. 5. At long times, one sees that the motion of the beads is constrained: they are trapped in Brownian cages whose size decreases when the cross-linking ratio increases. In Table I we report the value of δ^2, as obtained from the long-time behavior of $\langle \Delta_r^2(t) \rangle$ using Eqs. (20) or (21) depending on the value of δ^2. Also are given the values of $\langle \tau_c \rangle$ determined by fitting $\langle \Delta_r^2(t) \rangle$ to the equation [14]

$$\langle \Delta_r^2(t) \rangle = 6\,\delta^2[1-\exp[-(t/\tau_c)^\gamma]], \tag{22}$$

At short times, the beads motion tends again toward a subdiffusive behavior reflecting short time dynamics of the gel. We notice that, at short times, the beads in the less cross-linked gel appear to undergo a slower local diffusion as the mean squared displacement curve is the lowest.

It should be noted that, at present, the short time behavior of beads trapped in a viscoelastic medium gives rise to a debate. For instance, the issue on whether one recovers the diffusive behavior of probes in water or not is not yet resolved. In the present case, the experimental observation is likely due to the fact that a weakly cross-linked gel has a higher fraction of dangling ends and highly branched subparts that do not contribute to the elastic modulus but increase the local viscosity experienced by the particles. Second, we notice a slight shift between the measurements performed using DLS and DWS which cannot be accounted for by the slight difference of probe sizes. This is very likely due to the lack of reproducibility of the mechanical characteristics of the gel samples. Ideally, one would want to study the same gel with two very different concentrations of polystyrene spheres. This is not possible, and we had to prepare different samples for each technique. Unfortunately, these gels are close enough to the gel point that small deviations in the sample preparation conditions (e.g., added cross-linking) can cause some differences in the mechanical properties of the final sample.

We estimated the shear modulus μ of the gel, as probed by the particles, from the value of the maximum mean square displacement, $\langle \Delta r^2(t) \rangle$, arguing that the work necessary to move a bead of radius R by a distance Δr, inside a medium of elasticity is of thermal origin [4] so that

$$\mu = \frac{k_B T}{6\,\pi R\,\delta^2}, \tag{23}$$

$k_B T$ being the thermal energy. In fact, as discussed by Schnurr *et al.* [28], the above expression is strictly valid only at time scales which are short enough so that the solvent and the network move as one at scales large when compared with the mesh size of the network. In this limit the gel behaves as an incompressible fluid. An exact expression for longer time scales should include the contribution due to the compressional deformation since the stress in the solvent has time to relax completely as the network is deformed. The correction factor depends on the Poisson ratio and is negligible if the latter quantity is close to $\frac{1}{2}$. For polyacrylic acid gels prepared at a polymer concentration larger than those considered in this study [29], and for polyacrylamide gels in good solvent [30] the Poisson ratio was found to be close to $\frac{1}{3}$. With such value of the Poisson ratio the values of μ as determined by using Eq. (23) would be underestimated by about 12%, which is a small correction considering the large variation of μ as a function of the cross-linking ratio shown in Fig. 6.

When fitted to a power law, the elastic modulus variation with the cross-linking ratio yield an apparent scaling exponent of 2.91 ± 0.18. This result is not what one expects from the classical theory of rubber elasticity; however, this behavior, which has been observed previously, can be accounted for by the existence of dangling chains and unattached chains at low cross-link density and of trapped entanglements at high cross-link density. The former effect tends to decrease the shear modulus, the latter to increase it [31]. The discrepancy between the value of the local elastic modulus of the gel with $R_c = 5\times10^{-3}$ found using DLS and DWS might beexplained by the fact that the DLS measurement is clearly at the very limit of the resolution of this technique [cf. the inset in Fig. 1(a)]. This is precisely the reason why we resorted to DWS for these gels. The two samples were issued from different syntheses which introduce further uncertainty in the result.

We then compared the macroscopic measurement of the elastic modulus with optical measurements. We measured

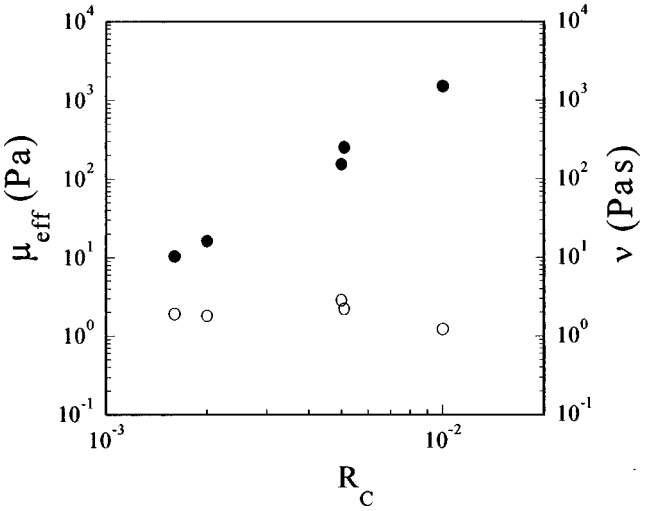

FIG. 6. Evolution of the local shear modulus μ as a function of the cross-linking ratio R_c (filled symbols). The local friction coefficient v is also plotted (open symbols).

the elastic modulus of a gel cross-linked at $R_c = 4 \times 10^{-3}$, with a Haake RS600 rheometer, and found that it did not vary with frequency between 2×10^{-2} and 2 Hz its value being 20 Pa. The comparison with macroscopic measurements is not straightforward. In fact, macroscopic measurements are usually performed by means of a uniaxial compression technique that provides the zero-frequency modulus. Measurements corresponding to the frequency domain accessible to the optical measurements are not possible with classical rheometers. A frequency-dependence of the storage modulus of weakly cross-linked gels is often observed, and this could account for the difference between macroscopic and microscopic measurements. Moreover, macroscopic dynamic measurements in cross-linked polymer gels are not straightforward, and are often marred by systematic errors which are very difficult to detect (e.g., surface defects and/or presence of a lubrication layer between the hydrogel and the plates of the rheometer), that lead to an underestimated value of the shear modulus.

The characteristic time required by a particle to explore its Brownian cage $\langle \tau_c \rangle$ is independent on the q value, as shown in Fig. 3(b), since it only depends on the characteristics of the sample and not on the scale of observation. It is possible to relate the average mean square displacement of the probe particles δ^2 and $\langle \tau_c \rangle$ to deduce the local friction coefficient:

$$v = \frac{k_B T \langle \tau_c \rangle}{6 \pi R \delta^2}. \tag{24}$$

Equation (24) is essentially a Stokes-Einstein relationship, v having the dimensions of a viscosity (Pa s). The values of δ^2, $\langle \tau_c \rangle$, v, and μ for the different systems we studied are summarized in Table I.

Contrary to the local shear modulus μ, the friction coefficient defined above is *independent* on the cross-linking ratio, as shown in Fig. 6. We note the satisfactory agreement of DWS and DLS results, especially considering the fact that size of the particles used in the two different types of experiments differed by about 20%. The local friction coefficient v reflects local relaxation processes of the polymer matrix which are not related to the cross-linking ratio of the polymer network. This result is not trivial and requires further investigation.

The mean square displacements of the particles could in principle be further analyzed by Laplace transform inversion of data to obtain the frequency-dependent storage and loss moduli of the matrix [4], which could be compared to macroscopic measurements. However, the numerical uncertainties of this procedure pose a problem. Also, an actual comparison would require reliable macroscopic measurements that are very difficult to obtain with classical rheometers in the same frequency range accessible to the optical measurements.

IV. CONCLUSION

We extended DWS to the case of nonergodic systems, and used this technique to measure the motion of colloidal particles trapped inside a chemically cross-linked gel. The inherent nongodicity of the scattering in these systems has to be addressed experimentally by performing explicit ensemble averages, or by using other averaging schemes. We measured the maximal amplitude of the motion of the particles, which we considered to act as viscoelastic probes of the gel matrix. From the mean square displacement we deduced the variation of the elastic modulus of cross-linked gels. Further work has to be done to compare the optical results to macroscopic measurements performed in the same frequency range. The results show that these scattering techniques are appropriate to investigate both dissipative short time properties and elastic moduli of permanently cross-linked gels. To probe the short time behavior, one has to use the DWS, whereas the choice of the technique for measuring the elastic modulus will depend of the value of this modulus. Upon increasing G, one turns successively to DLS, then to DWS in the transmission mode, and eventually to DWS in the backscattering mode.

Finally, one should note that such techniques provide new prospects for studying inhomogeneities of materials or following the local mechanical response of time-evolving systems such as associating systems or gels under swelling or deswelling.

ACKNOWLEDGMENTS

We thank F. Lequeux and J. F. Douglas for helpful comments on the paper, and D. J. Pine for fruitful discussions.

[1] H. Freundlich and W. Seifriz, Z. Phys. Chem., Stoechiom. Verwandtschaftsl. **104**, 233 (1922).
[2] S. C. Hunter, in *Proceedings of the Edinburgh Mathematical Society*, edited by F. F. Bonsall, W. D. Collins, D. Monk, A. D. Sands, and I. N. Sneddon (Oliver and Boyd, Edinburgh, 1969), Vol. 16.
[3] R. Nossal, Rubber Chem. Technol. **61**, 255 (1988).
[4] T. G. Mason and D. A. Weitz, Phys. Rev. Lett. **74**, 1250 (1995).
[5] F. Gittes, B. Schnurr, P. D. Olmsted, F. C. MacKintosh, and C. F. Schmidt, Phys. Rev. Lett. **79**, 3286 (1997).
[6] T. G. Mason, K. Ganesan, J. H. vanZanten, D. Wirtz, and S. C. Kuo, Phys. Rev. Lett. **79**, 3282 (1997).
[7] A. Palmer, B. Cha, and D. Wirtz, J. Polym. Sci., Part B: Polym. Phys. **36**, 3007 (1998).
[8] J.-P. Munch, P. Lemaréchal, S. J. Candau, and J. Herz, J. Phys. (France) **38**, 1499 (1977).
[9] A. Moussaid, J.-P. Munch, F. Schosseler, and S. J. Candau, J. Phys. II **1**, 637 (1995).
[10] J.-Z. Xue, D. J. Pine, S. T. Milner, X.-L. Wu, and P. M. Chaikin, Phys. Rev. A **46**, 6550 (1992).
[11] C. Rouf, J. Bastide, J. M. Pujol, F. Schosseler, and J.-P. Munch, Phys. Rev. Lett. **73**, 830 (1994).
[12] D. A. Weitz and D. J. Pine, in *Dynamic Light Scattering: The Method and Some Applications*, edited by W. Brown (Clarendon, Oxford, 1993), p. 652.
[13] D. A. Weitz, J. X. Zhu, D. J. Durian, H. Gang, and D. J. Pine, Phys. Scr. **T49**, 610 (1993).
[14] P. N. Pusey and W. Van Megen, Physica A **157**, 705 (1989).
[15] D. J. Pine, D. A. Weitz, J. X. Zhu, and E. Herbolzheimer, J. Phys. (France) **51**, 2101 (1990).
[16] E. Jakeman, in *Photon Correlation and Light Beating Spectroscopy*, edited by H. Z. Cummins and E. R. Pike (Plenum Press, New York, 1974), p. 75.
[17] B. J. Berne and R. Pecora, *Dynamic Light Scattering* (Wiley, New York, 1976).
[18] G. Nisato, Rachid Skouri, F. Schosseler, J.-P. Munch, and S. J. Candau, Faraday Discussion **101**, 133 (1995).
[19] R. Klucker and F. Schosseler, Macromolecules **30**, 4228 (1997).
[20] J. G. H. Joosten, J. McCarthy, and P. N. Pusey, Macromolecules **24**, 6690 (1991).
[21] P. Hébraud, F. Lequeux, J.-P. Munch, and D. J. Pine, Phys. Rev. Lett. **78**, 4657 (1997).
[22] Experiments performed on a bare gel (with no latex particles) showed that the frozen-in intensity is a negligible component of the total scattering intensity for the compositions considered.
[23] F. Ilmain and S. J. Candau, Prog. Colloid Polym. Sci. **79**, 172 (1989).
[24] F. Ilmain and S. J. Candau, Makromol. Chem., Macromol. Symp. **30**, 119 (1989).
[25] A. Moussaid, F. Schosseler, J.-P. Munch, and S. J. Candau, J. Phys. II **3**, 573 (1993).
[26] J. E. Martin, D. Adolf, and J. Wilcoxon, Phys. Rev. Lett. **61**, 2620 (1988).
[27] M. Delsanti and J.-P. Munch, J. Phys. II **4**, 265 (1994).
[28] B. Schnurr, F. Gittes, F. C. MacKintosh, and C. F. Schmidt, Macromolecules **30**, 7781 (1997).
[29] F. Schosseler, F. Ilmain, and S. J. Candau, Macromolecules **24**, 225 (1991).
[30] E. Geissler and A. M. Hecht, Macromolecules **13**, 1276 (1980).
[31] A. Silberberg, in *Polyelectrolyte Gels*, edited by R. S. Harland and R. K. Prud'homme (ACS, Washington, DC, 1992), Vol. 480, pp. 146 and 150.